Dynamic stability of one-dimensional models of fracture

Emily S.C. Ching
Department of Physics, The Chinese University of Hong Kong, Shatin, New Territories, Hong Kong

J.S. Langer
Institute for Theoretical Physics, University of California, Santa Barbara, California 93106-4030

Hiizu Nakanishi*
Department of Physics, Faculty of Science and Technology, Keio University, Yokohama 223, Japan
(Received 5 June 1995)

We examine the linear stability of steady-state propagating fracture in two one-dimensional models. Both of these models include a cohesive force at the crack tip; they differ only in that the dissipative mechanism is a frictional force in the first model and a viscosity in the second. Our strategy is to compute the linear response of this system to a spatially periodic perturbation. As expected, we find no dynamical instabilities in these models. However, we do find some interesting analytic properties of the response coefficient that we expect to be relevant to the analysis of more realistic two-dimensional models.

PACS number(s): 46.30.Nz, 62.20.Mk, 81.40.Np, 03.40.−t

I. INTRODUCTION

Studies of dynamic fracture, including our own work [1–3], ordinarily have stopped short of systematic stability analyses. For the most part, the basic ideas in this field have emerged from Yoffe's discovery [4] that the peak stresses near the tip of a running mode-I crack shift to the side at some critical velocity less than the Rayleigh speed. This observation, however, has not yet been converted into a demonstration that a crack actually becomes dynamically unstable against bending deformations at that or any other velocity.

There are intrinsic difficulties in carrying out conventional linear-stability analyses in fracture dynamics. In almost all mathematical models of fracture, the crack tip is a singularity in some displacement field, and the motion of the tip is governed nonlocally by the dynamics of that field. Moreover, a running crack is a driven, nonequilibrium system that must necessarily be examined in a moving frame of reference. Thus the linear-stability operator is not only nonlocal but also non-self-adjoint. In such situations, the eigenvalues of the stability operator, if they can be found at all, may not provide the most useful information and the reasons for this have been described by Trefethen *et al.* [5].

In this paper, we present a dynamic-stability analysis for two versions of a simple, one-dimensional model of a moving crack. The steady-state properties of this model have been described in an earlier publication [1]. Our main motivation for the present investigation has been to develop mathematical techniques for studying fracture stability. We do not expect there to be any dynamic instabilities in these models and, indeed, we have discovered none. But we have found some interesting mathematical results that we hope to exploit in our ongoing studies of fracture stability in higher dimensions.

The model to be considered here is defined by a differential equation of the form

$$\ddot{U}(x,t) = U''(x,t) - \mu^2 \left[U(x,t) - \tilde{\Delta}(x)\right] - f(x) - \phi(\dot{U}(x,t)). \tag{1.1}$$

Here, $U(x,t)$ is the crack opening displacement at position x and time t along the line of fracture, that is, along the x axis. Dots and primes denote differentiation with respect to t and x, respectively. We generally assume that the crack moves in the negative x direction. By definition, $U = 0$ along the unbroken region of the x axis, $x < x_{\rm tip}(t)$. Far behind the tip, $x \to +\infty$, the fully relaxed, broken configuration is $U(x) \approx \tilde{\Delta}(x)$.

In the absence of the terms denoted f and ϕ on the right-hand side, (1.1) is a massive wave equation in which position and time have been scaled so that the wave speed is unity. In higher-dimensional models, this wave speed would be the speed of a Rayleigh wave moving along the fracture surface. The "mass" μ is the inverse of a length that is roughly analogous to the width of a strip or the thickness of a plate in higher-dimensional fracture problems. In our units, μ^2 is the strength of an elastic coupling between the fracturing material and a fixed substrate at position $\tilde{\Delta}(x)$. Thus μ provides a long-wavelength or, equivalently, a low-frequency cutoff for the excitation spectrum of our one-dimensional elastic medium. The quantity $\mu^2\tilde{\Delta}(x)$ is the driving force for fracture. In the unbroken region where $U = 0$, the elastic energy available to drive the crack is $\mu^2\tilde{\Delta}^2/2$ per unit length.

Our strategy for a linear-stability analysis is to separate $\tilde{\Delta}(x)$ into two parts:

$$\tilde{\Delta}(x) = \Delta + \varepsilon(x), \tag{1.2}$$

*Present address: Department of Physics, Kyushu University 33, Fukuoka 812-81, Japan.

where Δ is the average driving force and $\varepsilon(x)$ is an infinitesimal perturbation. Note that we assume from the beginning that $\varepsilon(x)$ is a purely static perturbation. (It may be interesting in the future to look at the fully time-dependent problem in order to study the effects, for example, of thermal fluctuations or acoustic waves on crack motion.) So long as we restrict our attention to purely linear response, we can construct any perturbing force that we like by superimposing Fourier modes; therefore we write

$$\varepsilon(x) = \hat{\varepsilon}_m e^{imx}. \tag{1.3}$$

Our goal is to compute the linear response of the crack to this perturbation. Specifically, we define

$$\dot{x}_{\rm tip}(t) = -v - \hat{v}_m e^{-imvt}\ , \tag{1.4}$$

where v is the steady-state velocity at the unperturbed driving force Δ, and $-\hat{v}_m e^{-imvt}$ is the first-order response to the perturbation in (1.3). The response coefficient to be computed is

$$\chi(v,m) \equiv \frac{\hat{v}_m}{\hat{\varepsilon}_m}\ . \tag{1.5}$$

The function $f(x)$ in (1.1) is the cohesive force [6]. Ahead of the crack tip, where the crack is fully closed, $f(x)$ must just cancel the applied force:

$$f(x < x_{\rm tip}) \equiv f^{(-)}(x) = \begin{cases} \mu^2\tilde{\Delta}(x), & x < x_{\rm tip} \\ 0, & x > x_{\rm tip}. \end{cases} \tag{1.6}$$

When the crack starts opening at the tip, on the other hand, f becomes a function of U that, for simplicity, we take to have the form

$$f(x > x_{\rm tip}) = f_c\{U(x)\} = \begin{cases} f_0, & 0 < U < \delta \\ 0, & \delta < U. \end{cases} \tag{1.7}$$

Here, f_0 is the yield strength and δ is the range of the cohesive force. The fracture energy per unit length of crack is $\Gamma = f_0\delta$. Throughout this analysis, we shall assume that δ is a microscopic length, much smaller than any other length scale in the problem, and therefore, wherever possible, we shall work in the limit $\delta \to 0, f_0 \to \infty$ such that Γ remains constant. Note that the Griffith threshold occurs where the fracture energy Γ is equal to the stored elastic energy $\mu^2\tilde{\Delta}^2/2$; thus $\Delta_G = \sqrt{2\Gamma}/\mu$.

The final term in (1.1), $\phi(\dot{U})$, is the dissipative force that is needed in order that there be steady-state solutions above threshold, $\Delta > \Delta_G$, where the stored elastic energy exceeds the fracture energy. We shall consider two different cases, a frictional force with $\phi = 2\alpha\dot{U}$ and a viscous force with $\phi = -\eta\dot{U}''$. Because the friction model is somewhat simpler mathematically, we shall use it for setting up the stability analysis in Sec. II, and then shall describe the more interesting viscosity model in Sec. III. We end the paper with some concluding remarks in Sec. IV.

II. FRICTION MODEL: $\phi = 2\alpha\dot{U}$

The first step in our analysis is to transform the equation of motion (1.1) into a frame of reference that is moving in such a way that the tip of the crack is always at $x' = 0$. This transformation into a nonuniformly moving frame is essential because we must deal nonperturbatively with the singularity in $U(x,t)$ at $x = x_{\rm tip}(t)$. We set $x = x' + x_{\rm tip}(t)$ and then, for notational simplicity, let $x' \to x$. The result is

$$\ddot{U} - 2\dot{x}_{\rm tip}\dot{U}' + \dot{x}_{\rm tip}^2 U'' - \ddot{x}_{\rm tip}U' = U'' - \mu^2\left[U - \tilde{\Delta}(x + x_{\rm tip})\right] - f(x + x_{\rm tip}) - 2\alpha\dot{U} + 2\alpha\dot{x}_{\rm tip}U'. \tag{2.1}$$

We next write

$$U(x,t) = U_0(x) + U_1(x)\, e^{-imvt}, \tag{2.2}$$

where $U_0(x)$ is the zeroth-order, steady-state displacement at uniform driving force Δ, and $U_1(x)\, e^{-imvt}$ is the first-order correction due to the perturbation $\hat{\varepsilon}_m$.

In zeroth-order, the equation of motion becomes

$$\beta^2 U_0'' - \mu^2(U_0 - \Delta) - 2\alpha v\, U_0' - \mu^2\Delta\,[1 - \theta(x)]$$

$$-f_c\{U_0(x)\}\theta(x) = 0, \tag{2.3}$$

where $\beta^2 \equiv 1 - v^2$ and $\theta(x)$ is a step function that vanishes for $x < 0$ and is unity for $x > 0$. We can solve this equation immediately by Fourier transformation. Let $\hat{U}_0(k)$ denote the Fourier transform of $U_0(x)$. Then the transform of (2.3) is

$$\hat{F}_0(k)\,\hat{U}_0(k) = \frac{1}{\epsilon + ik}\left[\mu^2\Delta - f_0(1 - e^{-ikl})\right], \tag{2.4}$$

where ϵ is an infinitesimally small, positive number;

$$\hat{F}_0(k) = \beta^2k^2 + \mu^2 + 2i\alpha vk \equiv \beta^2(k - k^{(+)})(k - k^{(-)}) \tag{2.5}$$

and

$$k^{(\pm)} = -\frac{i\alpha v}{\beta^2} \pm i\sqrt{\left(\frac{\alpha v}{\beta^2}\right)^2 + \left(\frac{\mu}{\beta}\right)^2}. \tag{2.6}$$

The symbol l in (2.4) denotes the length of the cohesive zone, that is, l is the position where

$$U_0(l) = \delta, \tag{2.7}$$

beyond which the cohesive force drops to zero.

The function $U_0(x)$ vanishes for $x < 0$; accordingly, $\hat{U}_0(k)$ must be analytic in the lower half k plane. In order that there be no pole in $\hat{U}_0(k)$ at $k = k^{(-)}$, the right-hand side of (2.4) must vanish at that point:

$$\mu^2\Delta - f_0(1 - e^{-ik^{(-)}l}) = 0. \tag{2.8}$$

Equation (2.8) is, in effect, a solvability condition for (2.4). Then

$$U_0(x) = \frac{f_0}{\beta^2}\int \frac{dk}{2\pi}\frac{(e^{-ikl} - e^{-ik^{(-)}l})e^{ikx}}{(\epsilon + ik)(k - k^{(+)})(k - k^{(-)})}. \tag{2.9}$$

Equation (2.7) becomes

$$\delta = U_0(l) = \frac{f_0}{\beta^2}\int \frac{dk}{2\pi}\frac{(1 - e^{i(k-k^{(-)})l})}{(\epsilon + ik)(k - k^{(+)})(k - k^{(-)})} \approx \frac{f_0 l^2}{2\beta^2}. \tag{2.10}$$

To do the integration here, we assume that $k^{(\pm)}l \ll 1$ and then pick out the leading term in l by expanding the exponential to the order — 2 in this case — that gives an integrand that goes as k^{-1} at large k. Note that we can obtain the same result by evaluating $U_0''(0)$ directly from (2.3) and assuming $\mu^2\Delta \ll f_0$. In this limit, the solvability condition (2.8) becomes $\mu^2\Delta \approx ik^{(-)}l\,f_0$. We may think of these results as being exact in the limit $f_0 \to \infty$, $\delta \to 0$. For the friction model, the $k^{(\pm)}$ are nondivergent functions of α, v, and μ; they do not depend on f_0 or δ. Thus the solvability condition tells us that we can make l arbitrarily small by letting f_0 become large.

We complete the zeroth-order solution by eliminating l to find

$$\frac{\alpha}{\mu}\frac{v}{\beta} = \frac{(\Delta/\Delta_G)^2 - 1}{2(\Delta/\Delta_G)}. \tag{2.11}$$

This implicit formula for the steady-state v as a function of the driving force Δ shows that v rises from zero at $\Delta = \Delta_G$ and approaches unity as Δ becomes large. All of the above zero-order results may be found in Ref. [1]. In comparison to the techniques used in that paper, however, the Fourier methods used here seem simpler and more nearly analogous to the Wiener-Hopf techniques that are needed in two-dimensional versions of these problems.

The equation of motion in first order is

$$-\beta^2 U_1'' + 2v(\alpha - imv)U_1' + (\mu^2 - m^2v^2 - 2i\alpha mv)U_1 = -(2\alpha - imv)\hat{v}_m U_0' - 2v\hat{v}_m U_0'' - \left[f_c'(U_0)U_1 - \mu^2\hat{\varepsilon}_m e^{imx}\right]\theta(x). \tag{2.12}$$

In the next-to-last term,

$$-f_c'(U_0) = f_0\delta(U_0 - \delta) = \frac{f_0}{|U_0'(l)|}\delta(x - l) \approx \frac{\beta^2}{l}\delta(x - l), \tag{2.13}$$

where we have used a small-l approximation, $U_0'(l) \approx f_0 l/\beta^2$, analogous to the approximation used for $U_0(l)$ in (2.10).

The Fourier transform of (2.12) is

$$\hat{F}_1(k,m)\,\hat{U}_1(k) = k(2vk - mv - 2i\alpha)\,\hat{U}_0(k)\,\hat{v}_m + \frac{\mu^2\hat{\varepsilon}_m}{\epsilon + i(k - m)} + \frac{\beta^2}{l}U_1(l)\,e^{-ikl}, \tag{2.14}$$

where

$$\hat{F}_1(k,m) = k^2 - v^2(k - m)^2 + \mu^2 + 2i\alpha v(k - m) \equiv \beta^2(k - K^{(+)})(k - K^{(-)}). \tag{2.15}$$

In analogy to (2.6), we choose the $K^{(\pm)}$ to be the roots of $\hat{F}_1(k,m)$ whose imaginary parts are, respectively, positive and negative. (The two roots do lie on opposite sides of the real axis for all real m and $v < 1$.) Then the complete expression for $U_1(x)$ is

$$U_1(x) = \frac{1}{\beta^2}\int \frac{dk}{2\pi}\frac{e^{ikx}}{(k - K^{(+)})(k - K^{(-)})} \times\left[-\frac{(vm + 2i\alpha - 2vk)(e^{-ikl} - e^{-ik^{(-)}l})}{i(k - k^{(+)})(k - k^{(-)})}\frac{f_0\hat{v}_m}{\beta^2} + \frac{\mu^2\hat{\varepsilon}_m}{\epsilon + i(k - m)} + \frac{\beta^2}{l}U_1(l)\,e^{-ikl}\right]. \tag{2.16}$$

Solvability requires that the quantity in square brackets in (2.16) vanish at $k = K^{(-)}$ so that the integrand has no pole in the lower half plane at $k = K^{(-)}$. Use (2.12) or (2.16) to compute, for small l,

$$U_1(l) \approx \frac{l^2}{\beta^2}\left(\frac{v\hat{v}_m f_0}{\beta^2} - \frac{1}{2}\mu^2\hat{\varepsilon}_m\right). \tag{2.17}$$

Then the solvability condition becomes a linear relationship between $\hat{v}_m$ and $\hat{\varepsilon}_m$ that determines the response coefficient $\chi_\alpha(v,m)$:

$$\chi_\alpha^{-1}(v,m) \equiv \frac{\hat{\varepsilon}_m}{\hat{v}_m} = \frac{if_0 l}{\beta^2\mu^2}(K^{(-)} - m) \times\left[\frac{\beta^2(k^{(-)} - K^{(-)}) - mv^2}{mv}\right]. \tag{2.18}$$

The natural scale on which to measure $\chi_\alpha(v,m)$ is

$$\chi_\alpha(v,0) = \frac{dv}{d\Delta}, \tag{2.19}$$

that is, the response of the system to an infinitely long-wavelength perturbation.

First, let us examine m dependence of $\chi_\alpha(v,m)$ for real m. It is useful to start by noting that $\chi_\alpha(v,m)$ has a specially simple form in the particular case where $\alpha/\mu = 1$:

$$\chi_\alpha^{-1}(v,m) = \sqrt{2\Gamma}\,\frac{v+1}{\mu\beta^3}(1 - im/\mu). \tag{2.20}$$

The peak in the response is at $m = 0$ and its width is μ, independent of the velocity v.

For $\alpha/\mu = 0.1$, that is, for the case of small dissipation, the m dependences of $|\chi_\alpha(v,m)/\chi_\alpha(v,0)|$ and $\arg[\chi_\alpha(v,m)]$ are shown in Fig. 1 for three different velocities: v =0.01, 0.2, 0.9. In this limit of small α, the natural independent variable for Fig. 1 is the Lorentz-transformed frequency mv/β normalized to the low-frequency cutoff μ. This is just the frequency at which the nodes of the perturbation are passing the crack tip in the moving frame. In these units, the response becomes broader at higher velocities, but the peak always stays at $m = 0$, that is, there is no tendency toward a finite-wavenumber instability. The quantity $\arg[\chi_\alpha(v,m)]$ shown in Fig. 1(b) is the phase delay of the response, which shows more interesting structure. For the static perturbation ($m = 0$), the phase delay vanishes as it should, but it increases until the perturbation is resonant with the natural frequency μ, i.e., $vm/\beta = \mu$, and then decreases to the limiting value $\pi/2$. These features are basically those of a dissipationless system.

For a large value of the dissipation constant, $\alpha/\mu = 5$, the dynamics is controlled primarily by the friction; thus the natural independent variable is the frequency mv measured in units of the dissipation rate α. Our results for this case are shown in Fig. 2 for the same three values of v that we used in Fig. 1. The phase delay increases monotonically to the limiting value except for the case of extremely slow speed $v = 0.01$, in which there is a sharp rise at a small value of vm/α that is reminiscent of the behavior seen previously for small α/μ. We show this feature in the inset of Fig. 2(b), where the arguments are plotted for $v = 0.01$ and $\alpha/\mu = 0.1$, 1, and 5.

A second useful way to examine the formula (2.18) for $\chi_\alpha(v,m)$ is to look for poles in its analytic continuation into the complex m plane. These poles, if they exist, correspond to normal modes of the system. Poles at negative imaginary values of m correspond to stable, exponentially decaying modes; poles at positive imaginary values of m would imply instabilities. In the present case, the poles can be determined exactly. The factor $(K^{(-)} - m)$ in (2.18) vanishes at $m = -i\mu$ for all v, and the quantity in square brackets vanishes at $m = -2i\alpha/v$ except for the special case $\alpha/\mu = 1$ shown in (2.20) where the residue of the pole vanishes. We find no other poles, and therefore conclude that the friction model is entirely stable.

III. VISCOSITY MODEL: $\phi = -\eta\dot{U}''$

The basic equations for the viscosity model are the same as for the friction model except that 2α is replaced by $-\eta\,\partial^2/\partial x^2$. In the zeroth-order calculation, instead of (2.5), we have

$$\begin{aligned}\hat{F}_0(k) &= \beta^2k^2 + \mu^2 + i\eta vk^3 \\ &\equiv i\eta v(k-k_1)(k-k_2)(k-k_3),\end{aligned} \tag{3.1}$$

where the k_n, $n = 1,2,3$, are the three roots of $\hat{F}_0(k)$. We choose these roots so that, at small v, $k_1 \approx -k_2 \approx -i\mu$, and $k_3 \approx i/\eta v$. For any v, the root k_1 is always on the negative imaginary axis in the k plane and the other two roots on the positive imaginary axis. Then the solvability condition in zeroth order is precisely the same as (2.8):

$$\mu^2\Delta = f_0(1 - e^{-ik_1l}) \approx ik_1lf_0. \tag{3.2}$$

As before, the last expression in (3.2) is exact in the limit $f_0 \to \infty$, $\delta \to 0$ and, because k_1 is always finite, it implies that we may assume l to be arbitrarily small.

The complete expression for $U_0(x)$ is

$$U_0(x) = \frac{f_0}{\eta v}\int \frac{dk}{2\pi i}\,\frac{(e^{-ikl} - e^{-ik_1l})\,e^{ikx}}{(\epsilon + ik)(k-k_1)(k-k_2)(k-k_3)}. \tag{3.3}$$

In the limit of small l,

$$U_0(l) \approx f_0l^3/6\eta v. \tag{3.4}$$

We can obtain this result either by evaluating (3.3) or by

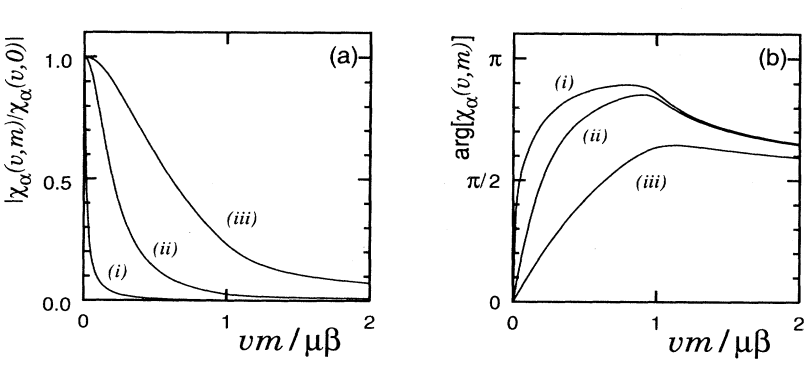

FIG. 1. m dependence of (a) amplitude and (b) argument of the response function $\chi_\alpha(v,m)$ for $\alpha/\mu = 0.1$ and (i) v =0.01, (ii) 0.2, and (iii) 0.9.

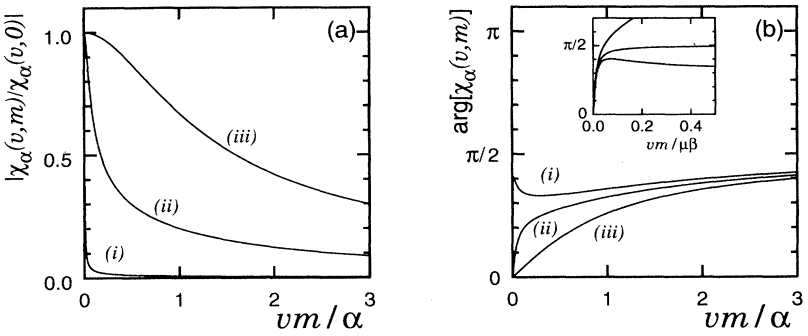

FIG. 2. m dependence of (a) amplitude and (b) argument of the response function $\chi_\alpha(v,m)$ for $\alpha/\mu = 5$ and (i) v =0.01, (ii) 0.2, and (iii) 0.9. The inset shows m dependence of the argument of $\chi_\alpha(v,m)$ for $v = 0.01$ and α/μ =5.0, 1.0, and 0.01 (from bottom to top).

computing $U_0'''(0)$ directly from the zeroth-order equation of motion. The validity of (3.4), however, requires that $k_n l \ll 1$ for all n, which is true everywhere except at $v \to 0$, where $k_3 \to \infty$. That is, the viscous length k_3^{-1} vanishes at the Griffith threshold while, for large but finite f_0, the cohesive length l remains finite. At all other values of v, we may safely assume that l is very much smaller than any other length in the system.

The first-order equations, analogous to (2.14) and (2.15), are

$$\hat{F}_1(k,m)\hat{U}_1(k) = k\,(2vk - mv - i\eta k^2)\,\hat{U}_0(k)\,\hat{v}_m + \frac{\mu^2\hat{\varepsilon}_m}{\epsilon + i(k-m)} + \frac{2\eta v}{l^2}U_1(l)\,e^{-ikl}, \tag{3.5}$$

where

$$\hat{F}_1(k,m) = k^2 - v^2(k-m)^2 + \mu^2 + i\eta v k^2(k-m) \equiv i\eta v(k-K_1)(k-K_2)(k-K_3). \tag{3.6}$$

Then the complete expression for $U_1(x)$ is

$$U_1(x) = \frac{1}{i\eta v}\int\frac{dk}{2\pi}\,\frac{e^{ikx}}{(k-K_1)(k-K_2)(k-K_3)} \times\left[-\frac{(2vk - vm - i\eta k^2)(e^{-ikl} - e^{-ik_1 l})}{\eta v\,(k-k_1)(k-k_2)(k-k_3)}f_0\hat{v}_m + \frac{\mu^2\hat{\varepsilon}_m}{\epsilon + i(k-m)} + \frac{2\eta v}{l^2}U_1(l)e^{-ikl}\right]. \tag{3.7}$$

For real m and $v < 1$, we find that only one of the three roots of (3.6), say K_1, has a negative imaginary part. Therefore solvability of the equation for U_1 requires that the quantity in square brackets in (3.7) vanish at $k = K_1$. In the limit of small l, and for $v \neq 0$,

$$U_1(l) \approx -\frac{l^3}{6\eta v}\left(\frac{f_0\hat{v}_m}{v} + \mu^2\hat{\varepsilon}_m\right). \tag{3.8}$$

As before, the solvability condition plus (3.8) becomes a linear relation between $\hat{v}_m$ and $\hat{\varepsilon}_m$ that determines the response coefficient:

$$\chi_\eta^{-1}(v,m) \equiv \frac{\hat{\varepsilon}_m}{\hat{v}_m} = -\frac{if_0 l}{\mu^2 v}(K_1 - m)\left(\frac{K_1 - k_1}{m} - \frac{1}{3}\right). \tag{3.9}$$

The quantities $|\chi_\eta(v,m)/\chi_\eta(v,0)|$ and $\arg[\chi_\eta(v,m)]$ are shown in Fig. 3 as functions of $vm/\mu\beta$ for $\eta\mu$ =0.01 and v =0.01, 0.2, 0.9. The main difference between the friction and viscosity models is that the width of the peak for large v in the viscosity model is broader than that in the friction model.

As in the case of the friction model, the factor $(K_1 - m)$ in (3.9) vanishes at $m = -i\mu$ for all v. The expression inside the square brackets gives another zero at

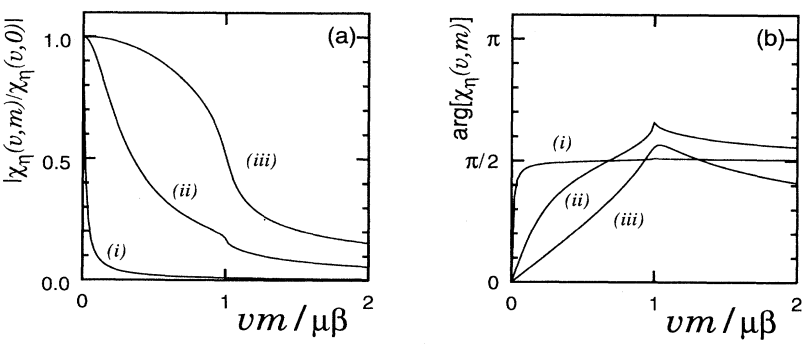

FIG. 3. m dependence of (a) amplitude and (b) argument of the response function $\chi_\eta(v,m)$ for $\eta\mu = 0.01$ and (i) v =0.01, (ii) 0.2, and (iii) 0.9.

$$m^* = -\frac{3i}{4\eta v}\left[1 - 4v^2 - 3\eta v|k_1| + \sqrt{(1 - 4v^2 - 3\eta v|k_1|)^2 + 16\eta v(1 + 2v^2)|k_1|}\right], \tag{3.10}$$

which is purely imaginary with a negative imaginary part and is on the branch of solutions for m^* for which the imaginary part of K_1 is negative. This implies that the system is stable against the perturbation. When η is small:

$$\eta v m^* \approx \begin{cases} -\dfrac{3i(1-4v^2)}{2}, & 0.5 - v \gg \sqrt{\eta\mu} \\ -\dfrac{3i}{2}\sqrt{\dfrac{6\eta\mu v}{\beta}}, & |0.5 - v| \ll \sqrt{\eta\mu} \\ -\dfrac{6i(1+2v^2)}{(4v^2-1)}\dfrac{\eta\mu v}{\beta}, & v - 0.5 \gg \sqrt{\eta\mu}. \end{cases} \tag{3.11}$$

The imaginary part of m^* is plotted in Fig. 4 as a function of v for various values of $\eta\mu$. The absolute value of m^* decreases significantly when $v \gtrsim 0.5$. This indicates a weakening in stability and should correspond to the fact that $|\chi_\eta(v,m)/\chi_\eta(v,0)|$ has a broader peak for large v.

IV. CONCLUDING REMARKS

We have carried out a systematic stability analysis of dynamic fracture in two simple one-dimensional models, the friction and the viscosity models, each with a different dissipative mechanism. Instead of attempting to find eigenvalues as in conventional linear-stability analyses, we have developed a different approach by evaluating the linear response of the crack to a small external perturbation of wave number m. The linear response coefficient, expressed as a function of m and the crack speed v, contains all the information pertaining to stability. The poles of the response coefficient, if they exist, correspond to normal modes of the system. Poles at negative imaginary values of m correspond to stable, exponentially decaying modes whose decay rate is the product of the velocity v and the magnitude of the imaginary part of m. On the other hand, poles at positive imaginary values of m would indicate instabilities. For the two models studied, two poles are found for the response coefficient, both at negative imaginary values of m; therefore we conclude that no dynamic instabilities exist in these one-dimensional models of fracture.

For both models, one of the poles of the response coefficient is at $m = -i\mu$ at all velocities v. Thus both models have a stable decaying mode with a decay rate $v\mu$. Because the length $1/\mu$ can be interpreted as the width of a strip or the thickness of a plate in higher-dimensional fracture problems, we suggest that this stable mode will become marginally stable (the pole will approach the real m axis) as the size of a higher-dimensional system becomes large.

For the friction model, the second pole is at $m = -2i\alpha/v$ corresponding to another stable mode with a decay rate 2α, independent of v. Thus the frictional force can always stabilize the propagation of fracture in this one-dimensional model, no matter what the velocity of propagation might be.

The viscosity model is mathematically more complex. The second pole is at m^* which, again, is on the negative imaginary m axis. The interesting feature is that the decay rate of the corresponding stable mode ($v|m^*|$) now depends on the velocity of fracture propagation as is shown in Fig. 4. It is larger for small v, decreases as v increases, and slightly increases again as v approaches the wave speed (unity). This behavior is the same for arbitrarily small values of η, so long as the viscous length scale ηv remains much longer than the (microscopic) length of the cohesive zone ℓ. The initial decrease of decay rate suggests a weakening in stability as the velocity of propagation increases, and is more dramatic when η is very small [see also (3.11)]. The minimum decay rate occurs at v in the range $0.5 - 0.8$, depending on the value of η, and its value is smaller for smaller η as expected.

Perhaps the most important general conclusion to be drawn from the present results is that it is absolutely essential to include some dissipative mechanism in dynamic stability analyses of fracture. Without dissipation, steady-state solutions exist only precisely at the Griffith threshold where the stored elastic energy is entirely taken up by the fracture energy as the crack extends. Thus it makes no sense to try to study stability by computing the response to some change in the driving force because only one special driving force is allowed. This behavior

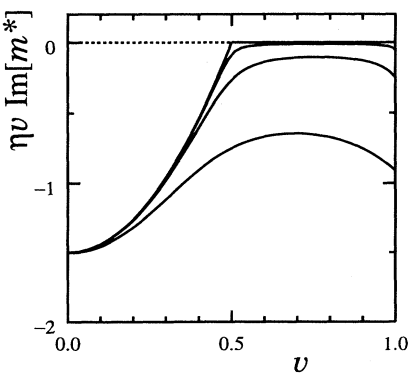

FIG. 4. v dependence of the imaginary part of one of the poles of $\chi_\eta(v,m)$ for $\eta\mu = +0$, 0.001, 0.01, and 0.1 (from top to bottom).

emerges clearly in our results. In the friction model, the pole in $\chi_\alpha(v,m)$ at $m = -2i\alpha/v$ would become an unphysical pole at $m = 0$ if we let α vanish at nonzero v. In the viscosity model, once we have taken the limit of a vanishingly small cohesive zone, our mathematics is well defined only for nonzero η, and the corresponding pole in $\chi_\eta(v,m)$ at $m = m^*$ stays well away from $m = 0$.

ACKNOWLEDGMENTS

E.S.C.C. acknowledges support by the Institute of Mathematical Sciences and the C.N. Yang Fund of the Chinese University of Hong Kong. J.S.L. has been supported by U.S. DOE Grant No. DE-FG03-84ER45108 and NSF Grant No. PHY89-04035.

[1] J.S. Langer, Phys. Rev. A **46**, 3123 (1992).
[2] J.S. Langer and H. Nakanishi, Phys. Rev. E **48**, 439 (1993).
[3] E.S.C. Ching, Phys. Rev. E **49**, 3382 (1994).
[4] E. Yoffe, Philos. Mag. **42**, 739 (1951).
[5] L.N. Trefethen, A.E. Trefethen, S.C. Reddy, and T.A. Driscoll, Science **261**, 578 (1993).
[6] See, e.g., L.B. Freund, *Dynamic Fracture Mechanics* (Cambridge University Press, New York, 1990) for more discussion on the cohesive force.